Comparison of Alternate Reactants for pM Level Cobalt Analysis in Seawater by the Use of Catalytic Voltammetry

Oliver Baars, Peter L. Croot*

FB2: Marine Biogeochemistry, IFM-GEOMAR, D-24105 Kiel, Germany
phone: +49 (431) 600-1510; fax: +49 (431) 600-4202
*e-mail: obaars@ifm-geomar.de

Received: January 4, 2011
Accepted: March 9, 2011

Abstract
The analysis of Cobalt (Co) at low pM concentrations in seawater with Adsorptive Cathodic Stripping Voltammetry involves high concentrations of sodium nitrite ($NaNO_2$) to enhance the signal in an electrocatalytic reaction. In this study we found three substitutes for $NaNO_2$ that critically affected the sensitivity. Optimisation of a method with potassium bromate ($KBrO_3$) resulted in an excellent detection limit (0.9 pM) after a 90 s adsorption period. Reactant concentration and consumption were 10× reduced compared to protocols with $NaNO_2$ and reagent blanks were lower. Accuracy and precision were verified with SAFe intercalibration standards and the method was applied using open ocean seawater samples. The reaction mechanism is discussed and differences to $NaNO_2$ are shown.

Keywords: Bromate, Electrocatalysis, Cobalt, Seawater, Stripping voltammetry

DOI: 10.1002/elan.201100003

Supporting Information for this article is available on the WWW under http://dx.doi.org/10.1002/elan.201100003

1 Introduction

For many organisms Cobalt (Co) is a bio-essential trace element and needed as the active metal centre in important vitamins (B_{12}) and enzymes (e.g. carbonic anhydrases, alkaline phosphatases) [1–4]. Low concentrations of Co make the analysis in environmental and natural samples challenging. Particularly in open ocean seawater samples measurements remain difficult (low pM concentrations). There are only few data available on the oceanographic distribution of Co and its speciation [5–11].

Trace Co analysis can be done using inductively coupled plasma mass spectrometry (ICP-MS) [12,13], atomic absorption spectroscopy (AAS) [14] or fluorometry in flow-injection analysis systems (FIA) [15]. With these instruments pre-concentration and/or matrix separation by solvent extraction [16–17], $Mg(OH)_2$ coprecipitation [18] or chelating resins [12–13] is necessary and can be connected with the risk of incomplete extraction, sample contamination or a complex experimental setup. Electrochemical systems combine minimized sample handling with a comparatively quick setup. The instrumentation is small and inexpensive. In addition information on the speciation of Co can be obtained [9–11]. Electrochemistry is therefore also highly suited for direct shipboard analysis.

The electrochemical detection of pM Co is performed by adsorptive cathodic stripping voltammetry (AdCSV, Table 1). Adsorptive ligands with dioximato functions are often used, e.g. dimethylglyoxime (DMG) [11,19] or 1,2-cyclohexanedione dioxime (Nioxime) [20]. The deprotonated species ($HDMG^-$) form electroactive square-planar bisdiozimato complexes with Co and Ni – $Co(HDMG)_2$ and $Ni(HDMG)_2$ – which adsorb to the surface of a mercury electrode. If sodium nitrite ($NaNO_2$) is added to the solution a strong peak increase (>40×) is observed during the cathodic stripping scan that results from regeneration of the electroactive compound by re-oxidation with NO_2^- in an electrocatalytic cycle (catalytic AdCSV) [21–23]. $NaNO_2$ is used in high concentrations (0.2–0.5 M) to reach the required sensitivity. Therefore high reactant consumption and elevated blanks are disadvantages of these methods [23]. Using Nioxime, Korolczuk et al. [24] reported a signal increase with addition of the surfactant cetyltrimethylammonium bromide (CTAB) due to either a catalytic reaction or enhanced adsorption of the Co complex, but the detection limit was not as good as with $NaNO_2$. No other reactants have been reported for the catalytic AdCSV detection of Co. While the choice of buffer and ligand has been subject of a number of studies (Table 1) the selection of the reactant $NaNO_2$ has not been addressed although alternatives might be available [25–28].

The substitution of $NaNO_2$ with other reactants could strongly influence the analytical performance and lead to benefits in sensitivity, reagent consumption or blank values and new mechanistic insights. Therefore, in this study, we tested alternate reactants and present three new substances that can lead to a great enhancement of the Co signal. Using potassium bromate ($KBrO_3$) as a substi-

Table 1. AdCSV methods for pM level Co analysis. ls: linear scan; DP: differential pulse; SW: square wave.

Ref.	Ligand	Reactant	$c_{Reactant}$ (mol/L)	Buffer	pH	Medium	*LOD* (pM)	Adsorption time (s)	Detection [d]
[9]	DMG	$NaNO_2$	0.225	EPPS	8	Seawater	<10	90	Fast Scan
[21]	DMG	$NaNO_2$	0.5–1.0	NH_3/NH_4Cl	9.3	H_2O	40	30	LS or DP
[23]	Nioxime	$NaNO_2$	0.5	NH_3/NH_4Cl	9.1	Seawater	3	60	DP
[24]	Nioxime	CTAB [a]	2.7×10^{-5}	PIPES		H_2O	17	60	DP
[29]	Diphenylglyoxime	$NaNO_2$	0.15	NH_3/NH_4Cl	9.3	Blood/H_2O	35	30–120	DP
[30]	2,2′-Bipyridine	$NaNO_2$	0.2	NH_3/NH_4Cl	8.6–9.3	H_2O	9.5	30	LS
[31]	Methylthymol blue	$NaNO_2$	0.8	NH_3/NH_4Cl	9	H_2O	85	60	DP
[32]	AADC [b]	$NaNO_2$	0.3	NH_3/NH_4Cl	10	H_2O	135	60	LS
[33]	PAR [c]	none	–	Phthalate	6	H_2O	50	50	DP
This study	DMG	$KBrO_3$	0.032	NH_3/NH_4Cl	9.2	Seawater	1	90	SW

[a] Cetyltrimethylammonium bromide; [b] Ammonium 2-Aminocyclohexene-1-dithiocarboxylate; [c] 4-(2-Pyridylazo)resorcinol; [d]

tute for $NaNO_2$ allowed to improve the detection limit at reduced reactant concentrations (Table 1). Based on these experiments new aspects of the catalysis mechanism are also discussed. Accuracy and precision of the method were evaluated by analysis of intercalibration samples (SAFe program). The method was then applied to Co analysis in seawater samples from the oligotrophic tropical Atlantic Ocean.

2 Experimental

2.1 Instruments and Reagents

Samples were UV digested with a Metrohm UV 705 system. The voltammetric system consisted of an Ecochemie PGSTAT30 connected to a VA663 voltammetric stand in the static mercury drop electrode mode. The reference electrode was a double junction, Ag/AgCl with a saturated AgCl internal solution and a salt bridge filled with 3 M KCl. The counter electrode was a platinum rod. The potentiostat was computer-controlled using GPES v4.9 (Eco Chemie) software. Samples were kept in a Teflon cell cup (Metrohm) and agitated with the inbuilt Teflon rod of the VA663. The solutions were purged with high purity nitrogen (Air Liquide, Nitrogen 5.0) connected to the VA663. An inoLab pH 720 (WTW) was used to determine pH values on the NBS scale. Standard trace metal clean techniques were used for handling and storage of reagents and samples (see also supplementary information). For the preparation of buffers and to acidify seawater samples, p.a. grade HCl (32%, Merck) was purified with a sub-boiling quartz still (Q-HCl, ~30%). Stock solutions of DMG (0.1 M, Fluka) were prepared in HPLC grade methanol (Fluka). Concentrated NH_4OH (25%, Fluka TraceSelect) was used for the ammonia buffer and adjusted with Q-HCl and 18 MΩ resistivity water (MQ) to yield a 5 M solution of pH = 9.2 ± 0.1. For the bromate stock solution, 3 g $KBrO_3$ (SigmaUltra or ACS grade, >99.8 %, Sigma-Aldrich) were dissolved in 50 mL MQ to give a 0.36 M solution. ACS grade $KBrO_3$ was cleaned by recrystallisation with 10^{-6} M EDTA in MQ at pH 7–8. The $KBrO_3$ solution was left overnight at 4°C and the crystals were washed with cold MQ and dried in a class-5 laminar airflow bench. All reagents were stored in Teflon bottles and refrigerated when not in use. The solutions were prepared new every 1–2 weeks. For details on sample collection and treatment the reader is referred to the Supporting Information.

2.2 Cobalt Determination

The seawater samples were 0.2 μm filtered and acidified to pH < 2 with Q-HCl. 10 mL sample aliquots were then UV digested for 2 h in previously cleaned Teflon capped quartz tubes. At the beginning of each day a standard Co sample was measured to ensure the system was clean and to monitor Co blanks. The 10 mL sample aliquots were transferred into the Teflon cell cup and the reagents were added in the order 0.11 M NH_3/NH_4Cl buffer (250 μL of the 5 M stock), 0.22×10^{-3} M DMG (25 μL of the 0.1 M stock) and 0.032 M $KBrO_3$ (1 mL of the 0.36 M stock). If non-acidified seawater samples were analysed, only 180 μL of the 5 M NH_3/NH_4Cl buffer was added (pH 9.2 ± 0.1). After each analysis the Teflon cell was thoroughly cleaned by rinsing with ethanol, dilute Q-HCl (pH < 2) and 10^{-4} M aqueous DMG. The voltammetric method included nitrogen purging for 200 s for the first measurement and 20 s after standard additions or for replicate measurements. A fresh Hg drop (VA 663 - drop size 2) was formed at the end of the purging period. During the deposition step the solution was stirred (stirrer speed 5) and a potential of −0.60 V was applied for 88 s. The potential was then switched to −1.025 V for 2 s to minimize the $Ni(HDMG)_2$ peak that could overlap with the Co signal. After a quiescence period of 10 s the potential was ramped from −0.60 V to −1.25 V using a square wave pulse modulation (frequency = 50 Hz; scan rate = 0.1275 V/s; pulse amplitude = 0.075 V; step potential = 2.55 mV). The baseline was recorded once before any standard additions were made by setting the deposition time to 0 s. The height of the Co peak was then determined after subtraction of the baseline scan from each voltammogram. The concentration of Co was calculated after 3 – 4 internal standard additions and each measure-

ment was run in duplicate. If not stated otherwise the final reagent concentrations used during the method optimisation experiments were: [NH_3 buffer] = 0.080 M (pH 9.1); [DMG] = 0.22 mM and [$KBrO_3$] = 0.032 M. The adsorption potential was set to −0.6 V for 88 s followed by a potential switch to −1.025 V for 2 s. After a quiescence time of 10 s a differential pulse (DP) modulation (Modulation Time = 0.01 s; Interval Time = 0.1 s; Step potential = 2.5 mV; Amplitude = 50 mV) was used in the potential scan from −0.6 V to −1.25 V. Each measurement was run in duplicate.

3 Results and Discussion

3.1 Reactant Selection

With the aim to increase sensitivities, lower reagent consumption or alleviate blank values and to get new insights into the catalysis mechanism $NaNO_2$ was substituted with a number of other reactants. These included inorganic reagents that have been used for the detection of other trace metals (hydroxylamine, NH_2OH/hydrogen peroxide, H_2O_2 / sodium chlorate, $NaClO_3$ / potassium bromate, $KBrO_3$) [25–28], sodium azide (NaN_3) and organic compounds that have been shown to be electrocatalytically reducible in waste water treatment related studies (trichloroacetate, TCA / trichloroethylene, TCE) [34–35]. The initial experimental conditions were oriented at protocols with $NaNO_2$ (Table 1). DMG was selected as adsorptive Co ligand and the pH was varied from 8.0–9.2 using 4-(2-hydroxyethyl)piperazine-1-propanesulfonate (EPPS) or ammonia buffers. The sensitivity (Δ *peak height*/$\Delta[Co^{2+}]$) was determined by internal Co^{2+} standard additions. Among the 7 reactants we found three that increased the sensitivity of the Co detection significantly: $KBrO_3$, NH_2OH and TCA. The concentration of each compound was adjusted with respect to sensitivity and background current (Table 2). Because of the strong peak amplification we suspected a catalytic mechanism in all cases.

If $KBrO_3$ was used as a reactant instead of $NaNO_2$ we found a 4× increase in the sensitivity while the concentration of $KBrO_3$ was more than 10× below typically used $NaNO_2$ concentrations. A baseline increase was observed at the end of the Co peak because of the uncatalysed BrO_3^- reduction. The peaks were slightly broader and anodically shifted (Table 2). Complications caused by the baseline increase and an interference between the Ni signal at −0.95 V and the Co peak at −1.13 V could be experimentally resolved (see also Section 3.6). Similar problems have also been reported in protocols with $NaNO_2$ [9,23]. Because of the extremely high sensitivity and low reagent consumption, the main work presented here deals with the optimisation of a method for the detection of pM Co in seawater using $KBrO_3$ instead of $NaNO_2$. $KBrO_3$ has been previously used for the catalytic AdCSV detection of other trace metals (e.g. Ti, V, Mo, Fe) [25–28].

If NH_2OH was compared to $NaNO_2$ the sensitivity was almost doubled at the same reactant concentration. Baseline, Co peak shape and half width ($w_{1/2}$) were similar to the signals with $NaNO_2$. NH_2OH can axially coordinate to $Co(HDMG)_2$ in a way NO_2^- binding was proposed [23,25] but the reduction of NH_2OH was energetically favoured (in alkaline solution: $E^0_{NH_2OH/NH_3} = +0.42$ V vs. $E^0_{NO_2^-/NH_3} = -0.16$ V). Therefore NH_2OH could be an important intermediate in the Co detection with $NaNO_2$. NH_2OH could also be a good alternative for $NaNO_2$ but it was needed in similarly high concentrations as $NaNO_2$. NH_2OH has been applied previously for the analysis of model solutions of niobium, ruthenium and tungsten [26] but we are aware of no application in natural samples.

Using TCA, the sensitivity was 10× higher than with $NaNO_2$ at more than 10× reduced concentrations. However, the baseline current was very high because of the direct reduction of TCA [36]. The Co peak was broad and shifted in the anodic direction so that it appeared close to the signal of $Ni(HDMG)_2$. Additionally a decrease in sensitivity could be observed at $[Co^{2+}] >$ 0.50 nM. Therefore we did not consider a further optimisation of the method with TCA. TCA has not been used previously in catalytic AdCSV.

We found that three diverse compounds ($KBrO_3$, NH_2OH and TCA) could be added to the range of reactants for Co detection with catalytic AdCSV while hitherto only $NaNO_2$ was known. Recently CTAB has also been suspected to be a catalytic reagent [24] but enhanced adsorption could also explain the signal increase

Table 2. Comparison of reactants for the electrocatalytic detection of Co. Conditions were: [DMG] = 0.25 mM; NH_3-buffer = 80 mM, a 90 s adsorption period at −0.6 V and detection with differential pulse voltammetry. Sensitivities were determined by internal Co standard additions. Peak positions and half widths ($w_{1/2}$) were recorded at $[Co^{2+}] = 0.45$ nM. The peak of $Ni(HDMG)_2$ appeared always at -0.95 ± 0.05 V.

Reactant [a]	$c_{Reactant}$ (M)	pH	Sensitivity (nA/nM)	Peak Pos. (V)	$w_{1/2}$ (V)
None	–	9.1	2.8	−1.16	0.040
$NaNO_2$	0.500	9.1	107	−1.18	0.044
$KBrO_3$	0.032	9.1	473	−1.13	0.090
NH_2OH	0.500	8.95	194	−1.17	0.036
TCA	0.015	9.2	9370	−1.00	0.133

[a] NaN_3, TCE, $NaClO_3$ and H_2O_2 did not show significant activity

in the presence of this surfactant. Therefore, it now appeared that there was a broad catalytic activity of Co bisdimethylglyoximate complexes that could be used for analytical purposes. This reactivity could be connected to the electrogeneration of $Co(I)(HDMG)_2$ species ($E^0_{Co(II)/Co(I)} < -0.9$ V; see also Section 3.5): Co(I) compounds are electron-rich, unstable and reactive [37–39]. These considerations contradicted a mechanism based on a Co(III)/Co(II) cycle which has been previously suggested with $NaNO_2$ [23].

3.2 Optimisation with $KBrO_3$: Solution Chemistry

3.2.1 BrO_3^- Concentration

After addition of BrO_3^- the peaks shifted from −1.16 V to −1.13 V because of the initiation of the electrocatalytic reaction. Due to the low solubility of BrO_3^- at room temperature a compromise needed to be reached between sample dilution and sensitivity gain. A baseline current increase because of the direct BrO_3^- reduction also needed to be considered. The ratio of peak height to baseline current approached a maximum at $[BrO_3^-] \geq$ 32 mM which was selected for the optimised protocol (Figure 1A).

3.2.2 Ligand Selection and Concentration

DMG and Nioxime have been successfully used with $NaNO_2$ and both ligands were compared at optimised concentrations using $KBrO_3$. The resulting sensitivities

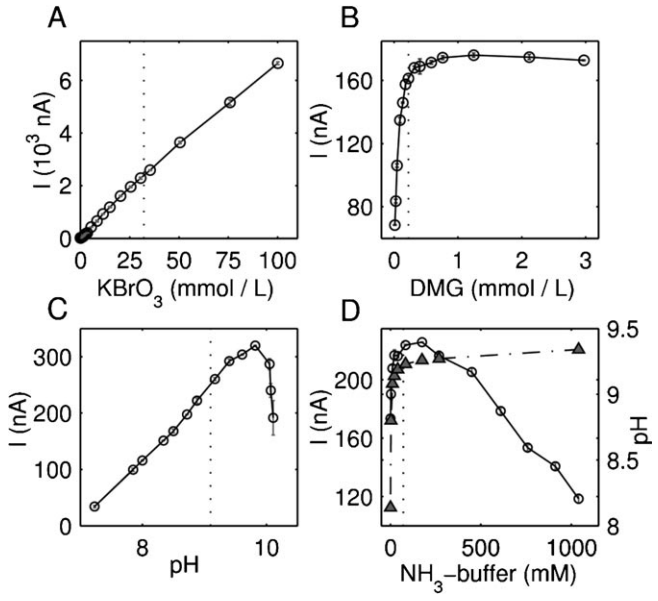

Fig. 1. Co peak heights as a function of (A) bromate, (B) DMG, (C) pH and (D) NH_3 buffer concentration (○ = Peak height and ▲ = pH) at $[Co^{2+}] = 0.45$ nM. The pH in C was adjusted by additions of Q-HCl or dilute KOH. Peak heights are corrected for dilution by the reagent additions. The selected concentrations are indicated by dashed vertical lines.

(S) were higher in the presence of DMG ([DMG] = 250 μM, $S = 741 \pm 13$ nA/nM) than with Nioxime ([Nioxime] = 15 μM, $S = 443 \pm 13$ nA/nM). In contrast, if $NaNO_2$ was used, Nioxime (659 ± 9 nA/nM) was better than DMG (145 ± 1 nA/nM). The opposite reactivity between $KBrO_3$ and $NaNO_2$ suggested different reaction mechanisms (Section 3.5). Figure 1B shows the dependence of the peak heights on the DMG concentration. DMG addition lead to a stabilisation of Co^{2+} and the peaks shifted ~8 mV in the cathodic direction. The observed [DMG] – current relationship indicated the adsorption of the 2 : 1 complex over the whole concentration range while formation of 1 : 1 or 3 : 1 complexes was negligible [11], [22].

3.3.3 pH

On the acidic side, the signal gain towards pH 9.8 could have been caused by a strong pH dependence of the Co-DMG complex stability ($\triangle \log K' / \triangle$pH ~2 [9]; the pK_A of DMG is 10.55 [40]) (Figure 1C). This was in agreement with a peak shift of −57 mV/pH. Weinzierl et al. made similar observations (−62 mV/pH) in the uncatalysed reaction [19] but linked this shift to an initial reversible $2H^+/2e^-$ reduction in $Co(HDMG)_2$. To prevent the formation of insoluble hydroxides in seawater (e.g. brucite) the pH was adjusted to 9.2. An NH_3 buffer was selected as readily available trace metal clean reagent. Note that the alternative use of a borate buffer or NaOH did not decrease or enhance sensitivities. This was in contrast to measurements with $NaNO_2$ where strong signal gains were observed in the presence of NH_3 buffers (see also Section 3.5). Connected to the pH changes following successive additions of the buffer (Figure 1D) the peak potentials shifted from −1.10 V to −1.40 V at high concentrations. A concentration of 0.080 M was sufficient to achieve nearly the optimal sensitivity in non-acidified seawater samples. For the analysis of acidified samples (pH 2) the concentration was increased to 0.110 M.

3.3 Optimisation of the Instrumental Parameters

Variations of the adsorption potential (Figure 2) lead to a Co signal decrease on the anodic side as the redox potential [41,42] of the $Co(II)/Co(III)(HDMG)_2$ couple was reached (−0.2 V to −0.3 V). In seawater the electrode surface was positively charged at this potential so that coulomb repulsion of $[Co(III)(HDMG)_2(NH_3)_2]^+$ species was a possible explanation. For Ni, only the divalent form was present over the whole potential range in agreement with constant stripping currents. To avoid side reactions at highly negative potentials the adsorption potential was set to −0.60 V. The observed Co peak heights were almost linearly related to the adsorption time between 0–600 s ($i_{45s} = 54$ nA; $i_{90s} = 108$ nA; $i_{180s} = 211$ nA; $i_{360s} = 381$ nA). The adsorption was carried out for 90 s which was sufficient for the detection of low pM Co. The parameters for square wave (SW), differential pulse (DP), staircase (SC) and sampled direct current (s-DC) were

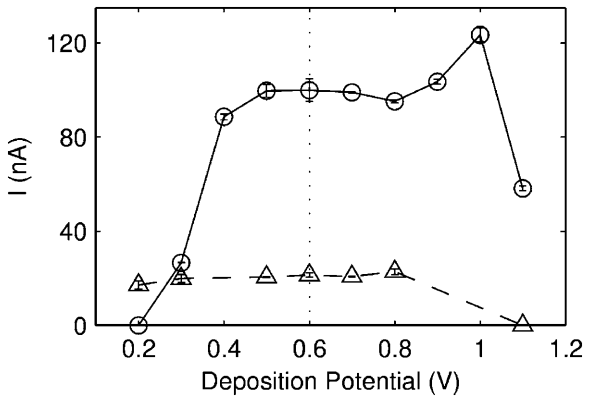

Fig. 2. Co (○) and Ni (△) peak height as a function of deposition potential ([Co^{2+}] = 0.20 nM; [Ni^{2+}] = 5.0 nM).

optimised for comparison. SW and DP were most sensitive if large pulse amplitudes ($\triangle E = 0.075$–0.150 V) were selected: SW > DP > SC > s-DC. Because of the high sensitivity and scan speed, a SW modulation was chosen.

3.4 Co redox State and Reagent Addition Order

After the destruction of stabilising ligands by UV digestion, hydrated Co(III) could be expected to be quickly reduced to Co(II) ($E^0_{Co(II)/Co(III)} = 1.84$ V) but upon addition of DMG, oxidation of $Co(II)(HDMG)_2$ became possible in the presence of oxygen. Experimentally, it could not be distinguished between the two redox states because of the reduction of $Co(III)(HDMG)_2$ to $Co(II)(HDMG)_2$ at the electrode. However, if $Co(III)(HDMG)_2$ was formed it did not affect the analytical results significantly: There was no difference between the results for a Co(II) spiked deoxygenated sample and a Co(II) spiked oxygenated sample that was analysed after 1 d. However it was noted that, if $KBrO_3$ or $NaNO_2$ was added to the solution prior to DMG, the Co recovery was low in UV and non-UV treated seawater (~60% if DMG was added within 5 minutes after $KBrO_3$, <10% after 1 d). The loss in detected Co could have resulted from Co(II) oxidation by BrO_3^- or NO_2^- to form inert Co(III) that could not be complexed by DMG. In seawater this reaction became possible if Co was embedded in strong complexes or an inorganic matrix [43]. The recovery loss was prevented with the following addition order: (1) NH_3-buffer, (2) DMG and (3) $KBrO_3$.

3.5 Reaction Mechanism

Scheme 1A illustrates the discussed aspects during the deposition step. Before the stripping step was started $Co(II)(HDMG)_2$ was adsorbed at the mercury electrode. There was no indication for a fast oxidation of Co(II) to $Co(III)(HDMG)_2$ by BrO_3^- in the baseline currents. The ~300× amplification of the Co peak with BrO_3^- pointed towards a catalytic mechanism and several observations were diagnostic of this reaction. If the scan speed (v) was increased using staircase voltammetry the peak height (i) did not increase to the same extend showing, that the number of electrons involved, was less at high scan rates and not constant, as expected in noncatalytic AdCSV [25]. A diffusion controlled catalytic reaction would be characterized by a linear relation in i vs. $v^{1/2}$ and i vs. $[BrO_3^-]^{1/2}$ [25]. The reaction with BrO_3^- appeared to be nondiffusion limited because the ratio $i/v^{1/2}$ decreased with increasing scan rate to reach a plateau and i increased linearly with $[BrO_3^-]$ (Figure 1A). The redox potentials of various Co(II)/Co(I) complexes have been observed in the range of the $Co(HDMG)_2$ peak [29–32, 37, 41] and Co(I) compounds are known to be catalytically reactive [37–39]. Therefore it was likely that a $1e^-$ reduction of $Co(II)(HDMG)_2$ produced an active Co(I) analogue that was quickly oxidized by BrO_3^- (Scheme 1B). BrO_2^- and BrO^- were probable instable intermediates in the reduction to the final product Br^- [44] and could have contributed to the signal, either by direct electrochemical reduction or by further oxidation of Co(I)-$(HDMG)_2$. At more negative potentials $Co(HDMG)_2$ was irreversibly reduced [45–47] which supposedly terminated the catalytic cycle.

During the optimisation differences between $KBrO_3$ and $NaNO_2$ were observed: (1) the sensitivities with $KBrO_3$ were higher using DMG while with $NaNO_2$, Nioxime was better, (2) the NH_3 buffer with $KBrO_3$ did not increase the sensitivity as observed with $NaNO_2$ [21,23] and (3) with $KBrO_3$ SW voltammetry was preferred while for $NaNO_2$ DP voltammetry was better. One explanation for these differences was the absence of axial coordination of BrO_3^- to the Co centre as shown also in the crystal structure of $[Co(H_2O)_6](BrO_3)_2$ [48]. With NO_2^- a direct coordination has been suggested to be important [22,23]. For example the NH_3 effect with NO_2^- has been ascribed to

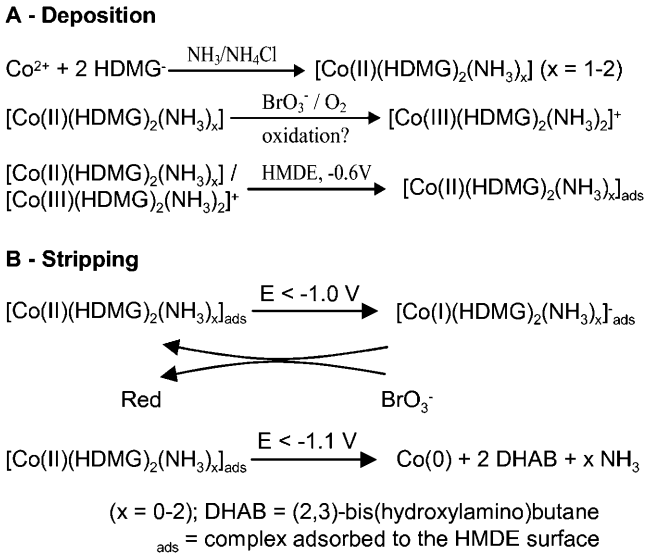

Scheme 1. Suggested mechanism for the catalytic AdCSV detection of Co with DMG and bromate.

the formation of active mixed complexes $[Co(HDMG)_2(NH_3)(NO_2)]$ [21,23].

3.6 Interferences

As illustrated in Figure 3A the baseline under the Co peak increased because of the direct reduction of BrO_3^-. Replicate voltammograms showed that the baseline was reproducible. In order to correct the baseline curvature a voltammogram was recorded using a deposition time of 0 s once for each sample. By subtraction of this voltammogram from the individual scans a flat baseline could be achieved in the vicinity of the Co signal (Figure 3B). A similar approach has been applied previously with DMG and $NaNO_2$ [9]. It was also possible to approximate the run of the baseline with an exponential function but this method was connected with reduced accuracy and precision and is not recommended at very low Co concentrations.

Ni forms strong DMG complexes with a reduction wave close to the Co signal. The Ni interference could be minimized with a potential jump to −1.025 V for 2 s at the end of the adsorption period. This procedure lead to an irreversible reduction of $Ni(HDMG)_2$ on the electrode surface [45] and a negligible Ni peak during the stripping step while the Co peak was not significantly affected. Other trace metal ions could also interfere with the Co determination. Cu and Fe competition was investigated specifically because DMG is known to bind to these metals [49,50]. The presence of 100 nM of each metal resulted in a peak decrease of ~5% for Co. The direct reduction of Zn^{2+} could produce a peak close to the observed Co signal but addition of 100 nM Zn^{2+} had no significant effect. Surface active substances are known to reduce the sensitivities by competitive adsorption to the electrode [20,23]. We made similar observations: the sensitivities in high dissolved organic matter seawater samples were up to 40% lower than in deep or UV digested samples. Intercalibration experiments (SAFe program, see GEOTRACES website) have additionally shown that currently available Co methods may not recover a large Co fraction in non-UV digested samples. UV digestion was also essential with this method (Figure 4).

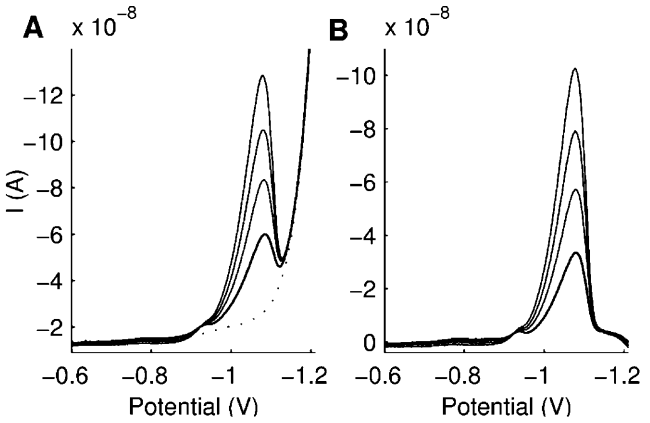

Fig. 3. Exemplary voltammograms using $KBrO_3$ for Co detection in an intercalibration sample (SAFe D2) with three internal standard additions of 33.0 pM (A). The dashed line is a voltammogram recorded after 0 s deposition time at the beginning of the measurements. Peak heights were determined after subtraction of the 0 s baseline voltammogram from the individual scans (B).

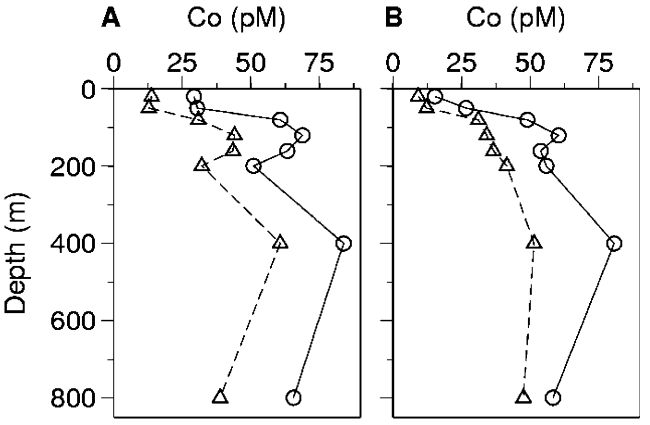

Fig. 4. Water column profiles of dissolved Co from the eastern tropical Atlantic ocean determined after UV treatment (○) and without UV treatment (△). The samples were collected at N 7° 40′ W 24° 13′ (A) and N 8° 1′ W 29° 59′ (B).

3.7 Blank Values

Low Co seawater was prepared by passing UV digested seawater over a pre-cleaned and conditioned Chelex-100 column [20]. Different qualities of $KBrO_3$ (SigmaUltra grade vs. ACS grade > 99.8%, Aldrich) were compared for Co impurities because at the time of the completion of this manuscript the SigmaUltra grade $KBrO_3$ was no longer available from the manufacturer. Using the purified seawater sample, the SigmaUltra grade $KBrO_3$ introduced no significant blank (< 5 pM). At these concentrations it was difficult to say whether the residual Co resulted from Co traces in the seawater sample or a small reagent blank. One ACS grade $KBrO_3$ was associated with elevated blanks (< 20 pM) while a second ACS grade batch introduced significant contamination (~150 pM). In this case the $KBrO_3$ was cleaned by re-crystallisation with EDTA. The reagent blank of the cleaned ACS grade $KBrO_3$ was < 5 pM. Using doubled concentrations of DMG or NH_3-buffer, no blank contribution was detected from these reagents. For DMG Co blanks have been reported in the literature, but it could be cleaned by recrystallisation from MQ with 10^{-3} M EDTA [51]. The reagent blanks were monitored by analysis of a low Co seawater sample each day.

3.8 Method Validation, Detection Limit, Linear Range

Accuracy and precision were evaluated using intercalibration samples from the GEOTRACES SAFe program (see GEOTRACES website). The samples were collected in

Table 3. Results with intercalibration samples. The intercalibration samples were provided by the GEOTRACES SAFe program. The latest SAFe consensus values are available on the GEOTRACES website. Errors are given as 1 standard deviation.

Sample	*n*	Co (pM)	+/−
SAFe S1 This study	10	7.5	1.1
SAFe S1 Consensus value		4.2	1.9
SAFe D2 This Study	10	44.9	2.4
SAFe D2 Consensus value		43.1	3.2

the northeast Pacific near the surface (SAFe S) and in 1000 m depth (SAFe D2). Assuming a negligible reagent blank our results for SAFe D2 were in perfect agreement with the consensus value from the intercalibration experiment (Table 3). For SAFe S there was a significant difference between the results but the value was within the range of concentrations determined by individual laboratories during the intercalibration and could be close to the real value. It was also possible that a small reagent blank or artefacts connected to the baseline subtraction procedure resulted in a small overestimation of the Co concentration. The reproducibility of the measurements was excellent. Eight replicate AdCSV scans with one SAFe S sample resulted in a relative standard deviation of 3.4 % and a detection limit (3× standard deviation) of 0.9 pM. The relative standard deviation of 7 independent determinations with SAFe S samples was 13 % and the resulting detection limit of the method was 2.7 pM which was likely connected to sample handling or wall effects. The sensitivity with UV digested seawater samples was 1100 ± 140 nA/nM (1 standard deviation). The proposed method allowed a detection limit significantly below the best method with $NaNO_2$ and DMG (< 10 pM, [9]) and a similar detection limit compared to the most sensitive previously published method with Nioxime and $NaNO_2$ (~3 pM) [23]. Using longer adsorption times the detection limit could be further reduced to sub pM values. The Co signal was linear between 0–7.5 nM (7 standard additions, $R^2 = 0.9999$) which included concentrations more than 10× above those found in open ocean and coastal seawater samples.

3.9 Open Ocean Seawater Profiles

The method was used to analyse Co concentrations in the tropical eastern Atlantic. Example profiles of dissolved Co determined after UV irradiation of the samples ("total Co") are shown in Figure 4. For comparison the plot includes results of Co analyses without the UV digestion step. The difference between the two datasets could be interpreted in context of Co speciation because it shows that a large fraction of Co was present in a non-reactive form that was probably associated with strong organic complexes.

4 Conclusions

The electrocatalytic reduction of diverse reactants by $Co(I)(HDMG)_2$ suggests that a variety of other compounds that could not be tested within this study could also come into question to enhance the Co peak. However it is important that a signal from the direct reduction of the reactant is well separated from the Co signal or that a baseline correction can be realized. Using the proposed method with $KBrO_3$ the detection limit for Co could be improved and the reactant concentration and consumption were strongly reduced facilitating routine Co measurements in the open ocean. With long adsorption times the analysis of sub pM Co concentrations becomes possible if sufficiently low blank values can be reached. In addition this method can be used to obtain information on the speciation of Co. Currently we are studying the Co speciation in the tropical eastern Atlantic using this method for the detection of reactive Co.

Acknowledgements

We thank the officers and crew of the *RV Meteor* for their support during the research expedition M80-2 and *M. Wilson* (RISE student) for assistance with the Co measurements. Comments and software by D. Omanović helped to improve this manuscript significantly. We also thank the reviewers for constructive suggestions. This work is a contribution of the Sonderforschungsbereich 754 "Climate – Biogeochemistry Interactions in the Tropical Ocean" (www.sfb754.de) which is supported by the *Deutsche Forschungsgemeinschaft* (*DFG*). Financial support for OB was provided by the *DFG* Antarctic Program SPP 1158 via Grants to PLC (CR145/10-1 & 10-2).

References

[1] M. J. Kendrick, M. T. May, M. J. Plishka, K. D. Robinson, *Metals in Biological Systems*, Ellis Horwood, London **1992**.
[2] W. G. Sunda, S. A. Huntsman, *Limnol. Oceanogr.* **1995**, *40*, 1404.
[3] C. Panzeca, A. J. Beck, K. Leblanc, G. T. Taylor, D. A. Hutchins, S. A. Sanudo-Wilhelmy, *Global Biogeochem. Cycles* **2008**, *22*.
[4] M. A. Saito, J. W. Moffett, S. W. Chisholm, J. B. Waterbury, *Limnol. Oceanogr.* **2002**, *47*, 1629.
[5] J. H. Martin, R. M. Gordon, S. Fitzwater, W. W. Broenkow, *Deep-Sea Res., Part A* **1989**, *36*, 649.
[6] M. A. Saito, J. W. Moffett, *Global Biogeochem. Cycles* **2004**, *18*.
[7] M. A. Saito, G. Rocap, J. W. Moffett, *Limnol. Oceanogr.* **2005**, *50*, 279.
[8] M. J. Ellwood, C. M.G. Van den Berg, M. Boye, M. Veldhuis, J. T. M. de Jong, H. J. W. de Baar, P. L. Croot, G. Kaltner, *Mar. Freshwater Res.* **2005**, *56*, 1069.

[9] M. A. Saito, J. W. Moffett, *Mar. Chem.* **2001**, *75*, 49.
[10] M. J. Ellwood, C. M. G. Van den Berg, *Mar. Chem.* **2001**, *75*, 33.
[11] H. Zhang, C. M. G. Van den Berg, R. Wollast, *Mar. Chem.* **1990**, *28*, 285.
[12] M. P. Hurst, K. W. Bruland, *Geochim. Cosmochim. Acta* **2008**, *72*, 395.
[13] Y. Sohrin, S. Urushihara, S. Nakatsuka, T. Kono, E. Higo, T. Minami, K. Norisuye, S. Umetani, *Anal. Chem.* **2008**, *80*, 6267.
[14] K. Kremling, P. Streu, *Deep-Sea Res., Part I* **2001**, *48*, 2541.
[15] V. Cannizzaro, A. R. Bowie, A. Sax, E. P. Achterberg, P. J. Worsfold, *Analyst* **2000**, *125*, 51.
[16] L. G. Danielsson, B. Magnusson, S. Westerlund, *Anal. Chim. Acta* **1978**, *98*, 47.
[17] K. W. Bruland, R. P. Franks, G. A. Knauer, J. H. Martin, *Anal. Chim. Acta* **1979**, *105*, 233.
[18] J. F. Wu, E. A. Boyle, *Anal. Chem.* **1997**, *69*, 2464.
[19] J. Weinzierl, F. Umland, *Fresenius' Z. Anal. Chem.* **1982**, *312*, 608.
[20] J. R. Donat, K. W. Bruland, *Anal. Chem.* **1988**, *60*, 240.
[21] A. Bobrowski, *Anal. Chem.* **1989**, *61*, 2178.
[22] A. Bobrowski, A. M. Bond, *Electroanalysis* **1992**, *4*, 975.
[23] M. Vega, C. M. G. Van den Berg, *Anal. Chem.* **1997**, *69*, 874.
[24] M. Korolczuk, A. Moroziewicz, M. Grabarczyk, K. Paluszek, *Talanta* **2005**, *65*, 1003.
[25] A. Bobrowski, J. Zarebski, *Electroanalysis* **2000**, *12*, 1177.
[26] P. M. Zaitsev, S. I. Zhdanov, T. D. Nikolaeva, *Russ. Chem. Rev.* **1982**, *51*, 552.
[27] M. Czae, J. Wang, *Talanta* **1999**, *50*, 921.
[28] G. P. Miropi, V. Anastasios, *Electroanalysis* **1993**, *5*, 355.
[29] B. Godlewska, J. Golimowski, A. Hulanicki, C. M. G. Van den Berg, *Analyst* **1995**, *120*, 143.
[30] Z. Gao, K. Siong Siow, *Talanta* **1996**, *43*, 255.
[31] A. Safavi, E. Shams, *Talanta* **2000**, *51*, 1117.
[32] A. A. Ensafi, S. Abbasi, *Anal. Sci.* **2000**, *16*, 377.
[33] L. Hosseinzadeh, S. Abbasi, H. Khani, Z. Khani, *Transition Met. Chem.* **2009**, *34*, 425.
[34] R. Zhuang, F. Jian, K. Wang, *J. Mol. Struct.* **2009**, *938*, 254.
[35] A. Alatorre Ordaz, J. Manriquez Rocha, F. J. Acevedo Aguilar, S. Gutierrez Granados, F. Bedioui, *Analusis* **2000**, *28*, 238.
[36] G. Torsi, P. Papoff, *Fresenius' J. Anal. Chem.* **1966**, *224*, 130.
[37] O. Buriez, E. Labbe, J. Perichon, *J. Electronanal. Chem.* **2006**, *593*, 99.
[38] W. Kaim, B. Schwederski, *Bioanorganische Chemie*, Teubner Verlag, Wiesbaden **2005**, Vol. 4.
[39] J. K. Stille, K. S. Y. Lau, *Accounts Chem. Res.* **1977**, *10*, 434.
[40] E. K. Astakhova, *Ph.D. Thesis*, Moscow **1964**.
[41] I. Adaev, T. Korostoshevskaya, V. Novikov, T. Lysyak, *Russ. J. Electrochem.* **2005**, *41*, 1125.
[42] C. M. Elliott, E. Hershenhart, R. G. Finke, B. L. Smith, *J. Am. Chem. Soc.* **1981**, *103*, 5558.
[43] A. J. Bard, R. Parsons, J. Jordan, *Standard Potentials in Aqueous Solution*, Marcel Dekker, New York **1985**.
[44] *Inorganic Reaction Mechanisms,* Vol. 13 (Ed: J. O. Edwards), Wiley Interscience, New York **1970**.
[45] F. Ma, D. Jagner, L. Renman, *Anal. Chem.* **1997**, *69*, 1782.
[46] L. A. M. Baxter, A. Bobrowski, A. M. Bond, G. A. Heath, R. L. Paul, R. Mrzljak, J. Zarebski, *Anal. Chem.* **1998**, *70*, 1312.
[47] D. V. Vukomanovic, J. A. Page, G. W. vanLoon, *Anal. Chem.* **1996**, *68*, 829.
[48] A. C. Blackburn, J. C. Gallucci, R. E. Gerkin, *Acta Crystallogr. Sect. B, Struct. Sci.* **1990**, *46*, 712.
[49] C. V. Banks, S. Anderson, *Inorg. Chem.* **1963**, *2*, 112.
[50] G. Sitaramarah, M. L. V. Rao, *Curr. Sci.* **1957**, *26*, 176.
[51] M. A. Saito, J. W. Moffett, *Geochim. Cosmochim. Acta* **2002**, *66*, 1943.

